Journal of Magnetic Resonance 323 (2021) 106888

Contents lists available at ScienceDirect

Journal of Magnetic Resonance

journal homepage: www.elsevier.com/locate/jmr

# Hyperpolarization transfer pathways in inorganic materials

Snædís Björgvinsdóttir, Pinelopi Moutzouri, Brennan J. Walder, Nicolas Matthey, Lyndon Emsley *

*Institut des Sciences et Ingénierie Chimiques, Ecole Polytechnique Fédérale de Lausanne (EPFL), CH-1015 Lausanne, Switzerland*

ARTICLE INFO

*Article history:*
Received 19 August 2020
Revised 30 October 2020
Accepted 1 December 2020
Available online 5 December 2020

*Keywords:*
Solid-state NMR
Dynamic nuclear polarization
Spin diffusion

ABSTRACT

Dynamic nuclear polarization can be used to hyperpolarize the bulk of proton-free inorganic materials in magic angle spinning NMR experiments. The hyperpolarization is generated on the surface of the material with incipient wetness impregnation and from there it is propagated towards the bulk through homonuclear spin diffusion between weakly magnetic nuclei. This method can provide significant gains in sensitivity for MAS NMR spectra of bulk inorganic compounds, but the pathways of the magnetization transfer into the material have not previously been elucidated. Here we show how two-dimensional experiments can be used to study spin diffusion from the surface of a material towards the bulk. We find that hyperpolarization can be efficiently relayed from surface sites to multiple bulk sites simultaneously, and that the bulk sites also engage in rapid polarization exchange between themselves. We also show evidence that the surface peaks can exchange polarization between different sites in cases of disorder.



## 1. Introduction

Solid-state NMR is routinely used to obtain information about the atomic level structure and properties of both organic and inorganic materials. The application of NMR can sometimes be limited by low sensitivity, caused by low concentration or low gyromagnetic ratio of the magnetically active nuclei. This is especially true in cases where the material does not contain protons, as it eliminates the possibility of increasing sensitivity by cross-polarization (CP). Additionally, many rigid solids have spin-lattice relaxation times that are long, which further limits sensitivity.

Dynamic nuclear polarization (DNP) enhanced magic-angle-spinning (MAS) NMR using incipient wetness impregnation has been demonstrated to provide improvements in sensitivity for a range of solid materials [1–3]. Most commonly, the target material is wetted with a frozen solution of a radical which serves as the polarizing agent. The large polarization of the unpaired electrons is primarily transferred from the exogenous polarizing agent to nearby protons with microwave irradiation at the EPR frequency. From there, spontaneous $^{1}$H-$^{1}$H spin diffusion propagates the hyperpolarization throughout the frozen solution and into the target, provided the target material is proton-containing. This process is referred to as polarization relay. The hyperpolarization can then be transferred to less sensitive nuclei, such as $^{13}$C and $^{15}$N, by CP [4–6]. Relayed DNP based on $^{1}$H-$^{1}$H spin diffusion has, for example, been used to characterize pharmaceuticals, measure domain sizes in materials, and determine the structure of crystalline nanoparticles [7,8]. When the substrate does not contain protons, as is often the case for inorganic solids, the hyperpolarization generated by incipient wetness impregnation DNP is focused at the surface of the material, resulting in DNP surface enhanced NMR spectra (DNP-SENS) [9].

We recently introduced a method to hyperpolarize the bulk of proton-free inorganic materials using DNP, resulting in considerable sensitivity enhancements in solid-state MAS NMR experiments [10,11]. This is achieved by generating or transferring hyperpolarization to weakly magnetic nuclei at or near the surface of the material [9] and then allowing homonuclear spin diffusion to transport the hyperpolarization into the bulk of the material. Homonuclear spin diffusion between nuclei such as $^{31}$P and $^{119}$Sn is considerably slower than that of protons, mainly due to low concentration of magnetically active nuclei and low gyromagnetic ratio. Furthermore, the already weak dipolar interactions are further averaged out under MAS. Since the first-order homonuclear dipolar Hamiltonian of a many-spin network (i.e. three or more spins that are not colinear) is homogeneous, diffusivity is approximately proportional to $\nu_r^{-1}$, and is only truly zero in the limit where the MAS rate tends to infinity [12,13]. On the other hand, when nuclear $T_1$ relaxation rates are long, as is often the case for rigid solids, even slow spin diffusion can efficiently transfer hyperpolarization from surface to bulk. We have demonstrated this for $^{119}$Sn spectra of $SnO_2$, $^{31}$P spectra of GaP, $^{113}$Cd spectra of CdTe and $^{29}$Si spectra of $SiO_2$ (α-quartz), with gains in overall sensitivity

* Corresponding author.

https://doi.org/10.1016/j.jmr.2020.106888
1090-7807/

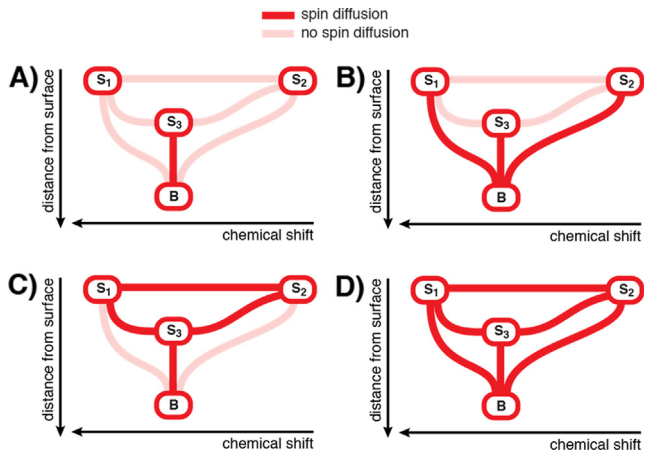


**Fig. 1.** Schematic representation of possible hyperpolarization transfer pathways from three surface sites ($S_1$, $S_2$ and $S_3$) to bulk (B). $S_3$ has the same chemical shift as the bulk. (A) Only transfer from $S_3$ to B. (B) Transfer from all three surface sites to bulk. (C) Exchange between all three surface sites, and transfer from $S_3$ to B. (D) Transfer between all sites in the system.

of up to a factor 85 so far, corresponding to an acceleration in acquisition times by a factor of over 7000. These materials, however, all have only a single isotropic chemical shift in the bulk. As such, the question remains of how hyperpolarization may be relayed through distinct surface and bulk species: is the transport of hyperpolarization into the bulk carried across different bulk species on distinct *hyperpolarization transfer pathways*, and is the net accumulation of polarization site dependent?

Fig. 1 shows a schematic representation of four different transfer paths. The dominance of specific hyperpolarization transfer pathways and polarization ratios of bulk sites that differ from unity might be anticipated due to numerous site-specific factors which modulate the rate of spin diffusion. Large chemical shift differences are expected to slow down spin diffusion, roughly as the inverse square of the difference between the isotropic chemical shifts but with significant additional modulation by homonuclear *J*-coupling, chemical shift anisotropy, the relative orientation of anisotropic principal axis systems (including those of nuclei to which the site is coupled), all further complicated by rotational resonance effects introduced by MAS [14,15]. The analysis is entirely nontrivial and differences in accumulated polarization can be readily envisaged.

Here we extend the method of hyperpolarization by relay from the surface to compounds that have more than one isotropic chemical shift in the bulk. We make use of two-dimensional experiments to probe hyperpolarization transfer pathways into the bulk beginning at the surface for the $^{119}$Sn nuclei of $SnO_2$ and the $^{31}$P nuclei of GaP, $Sn_2P_2O_7$ and $K_4P_2O_7$. We find that hyperpolarization can be efficiently relayed from surface sites to multiple sites in the bulk simultaneously, even when chemical shift differences are relatively large. We also see that polarization of the bulk sites exchanges rapidly between sites and polarization from multiple surface sites can be relayed simultaneously into bulk. In addition, we show evidence that disordered surface sites can exchange polarization between themselves.

## 2. Experimental methods

Solid-state NMR spectra were collected on a 9.4 T Bruker Avance III spectrometer coupled with a 263 GHz gyrotron microwave source [16]. The spectra were collected at a MAS rate of 8 kHz and a temperature of around 100 K using 3.2 mm sapphire rotors and a low-temperature MAS DNP probe. For efficient spin locking during cross-polarization, a 100 kHz rf field amplitude was applied on the X channel unless otherwise specified. The $^1$H rf field amplitude was ramped up from 90% during CP to improve polarization transfer efficiency. Presaturation pulses were used on both $^1$H and X channels in all experiments. See SI for further details.

$Sn_2P_2O_7$ (abcr), $SnO_2$ (abcr) and $K_4P_2O_7$ (Sigma Aldrich) were ground by hand and GaP flakes (abcr) were crushed in a mixer mill with a stainless-steel ball. The resulting micrometer sized particles (see SEM images in SI) were impregnated with a 16 mM solution of TEKPol [17] in 1,1,2,2-tetrachloroethane (TCE) [9,18]. The formulation ratio was 30–55 mg of powdered solid to 10 μL of radical solution, depending on the solid. Tin pyrophosphate was heated at 250 °C overnight before impregnating. To improve DNP enhancements, the packed samples were deoxygenated by rapid freezing and subsequent thawing by three insert-eject cycles [19,20].

DMFIT was used for spectral deconvolution [21].

## 3. Results and discussion

### 3.1. Hyperpolarization relay from the surface

#### 3.1.1. $^{31}$P spin diffusion in tin pyrophosphate

We begin our investigation of relay into multiple bulk sites by considering tin pyrophosphate, $Sn_2P_2O_7$. The material has a triclinic crystal structure with two distinct bulk phosphorous sites [22], leading to a $^{31}$P MAS spectrum showing two distinct signals, at −11.6 ppm and −15.4 ppm, occurring in a 1:1 ratio [23]. To monitor the transport of $^{31}$P magnetization, the powdered solid is impregnated with a radical containing solution and hyperpolarization is generated on protons in the wetting phase by continuous microwave irradiation. Hyperpolarization is then transferred to $^{31}$P nuclei near the surface of the tin pyrophosphate particle with cross-polarization. After CP, a flip-back storage pulse puts the $^{31}$P magnetization along the z direction, where spontaneous $^{31}$P homonuclear spin diffusion may transport magnetization between different phosphorous species during a delay $\tau_m$. A final 90° pulse

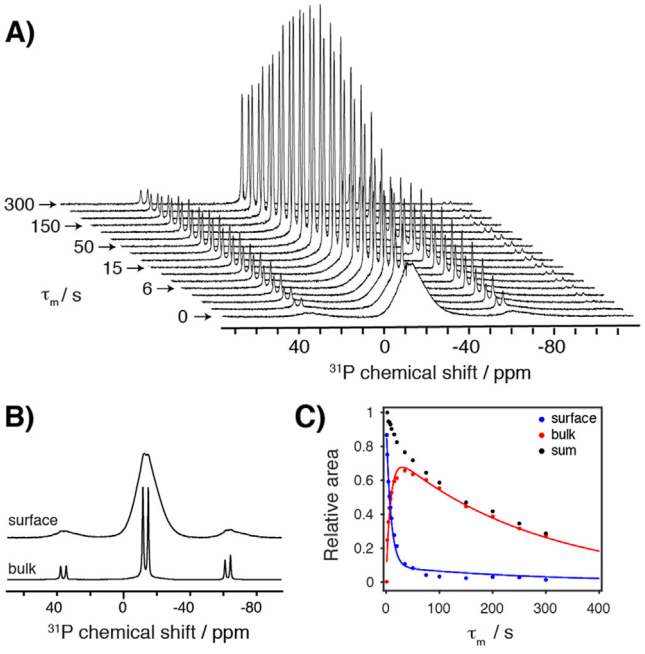


**Fig. 2.** (A) DNP enhanced $^{31}$P CP spectra of $Sn_2P_2O_7$ acquired as a function of $\tau_m$. (B) $^1$H-$^{31}$P CP surface spectrum, and direct $^{31}$P bulk spectrum of $Sn_2P_2O_7$. (C) $^{31}$P peak areas for the surface and bulk sites as a function of time. The solid lines are fits to the data based on an exchange model as described in the text.

then puts the magnetization back in the transverse plane before acquisition [10]. Fig. 2A shows such DNP enhanced $^{1}$H-$^{31}$P CP spectra of $Sn_2P_2O_7$, acquired at 8 kHz MAS and 100 K, collected for different values of $\tau_m$. We see that for $\tau_m$ = 0 only the surface is polarized, yielding a broad spectrum extending from around -10 ppm to about -30 ppm. There is almost no signal from the bulk, as can be seen in the comparison shown in Fig. 2B, where the $^{1}$H-$^{31}$P CP surface spectrum is compared to the direct $^{31}$P bulk spectrum of $Sn_2P_2O_7$. In line with previous observations on materials with only one bulk species, we then see that when $\tau_m$ is increased, the bulk signal intensity increases, while surface signals concomitantly diminish. Fig. 2C shows the integrals of the surface and bulk sites, from which we see that the total signal volume diminishes in a way consistent with longitudinal relaxation, implying the bulk sites have picked up enhanced polarization from the surface sites. This result unambiguously demonstrates that the transfer of polarization from the surface to the two bulk sites occurs spontaneously, and that they are polarized on the same timescale. However, this experiment does not provide sufficient information to infer many details about the relevant polarization transfer pathways.

This kind of hyperpolarization relay has been simulated previously using numerical models based on diffusion [8,10]. The diffusion model assumes that the transfer of polarization behaves like a thermal diffusion process, and it contains spatially juxtaposed components: typically a hyperpolarization source, and a target which gets hyperpolarized by relay. These models are very powerful tools to determine the spatial arrangement of different components [7,24,25]. However, in many inorganic solids, not only can there be a separation on the spin diffusion length scale between surface sites and the bulk, but there is often also frequency separation in the spectra between magnetically inequivalent sites that are neighbors on the atomic scale. In these cases, setting up a full spatial model of the system is not straightforward, and is not necessarily required if the objective is to characterize the overall rates of flow of magnetization between the different chemical shifts. To address this problem here, we use a simplified kinetic model to approximate the dynamics.

In a simplified model, where a surface and bulk peak are in exchange, the peak volumes can be fit to the modified Bloch equations for a two-site exchange [26,27]:

$$\mathrm{S(surface)} \underset{k_{BS}}{\overset{k_{SB}}{\rightleftarrows}} \mathrm{B(bulk)} \tag{1}$$

$$\frac{dV_S}{dt} = \frac{V_S^{eq} - V_S(t)}{T_{1,S}} - k_{SB}V_S(t) + k_{BS}V_B(t) \tag{2}$$

$$\frac{dV_B}{dt} = \frac{V_B^{eq} - V_B(t)}{T_{1,B}} + k_{SB}V_S(t) - k_{BS}V_B(t) \tag{3}$$

where $t$ is time; $V_S$ and $V_B$ are the instantaneous volume magnetizations of the $^{31}$P nuclei at the surface and in the bulk, which are proportional to the integrated signal intensities; $k_{SB}$ and $k_{BS}$ are the observed exchange rate constants; $T_1$ are the spin lattice relaxation rates; and $V^{eq}$ are the equilibrium volume magnetizations (at $t = \infty$) of the surface and bulk. In the CP experiment used here, phase cycling is such that the magnetization decays to 0, $V^{eq}$ = 0.

We use this model to fit the curves shown in Fig. 2C, assuming that the two bulk sites are one site (since they have the same growth). The observed rate constants obtained from the fits are $k_{SB}$ = 0.09 s$^{-1}$ and $k_{BS}$ = 0.01 s$^{-1}$ (see SI for details). While the microscopic interpretation of the observed rate constants in terms of spin flip-flops is not straightforward, they do provide a convenient way to quantify the overall flow of hyperpolarization from surface to bulk and the polarization exchange between the different sites in the spectra, which is the question addressed here. The observed rates do not directly correspond to spin diffusion rates between the different regions of the sample, which can only be extracted (in principle) using constitutive models taking into account the detailed geometry of the samples [24].

The $^{31}$P hyperpolarization transfer pathways from surface to bulk can alternatively be probed in with a two-dimensional experiment in the manner of classic exchange spectroscopy [28–30]. In the DNP enhanced 2D CP EXSY experiment, shown in Fig. 3A, the effect of spin diffusion during the mixing period, $\tau_m$, is to create off-diagonal intensities when magnetization is transferred to $^{31}$P sites with chemical shifts that differ from the original species. An unusual aspect of this application of exchange spectroscopy is that the initial condition is very far from equilibrium, since the surface is hyperpolarized. Therefore, the flow of polarization will not be equal in both directions, and the 2D experiment primarily contains information about the forward (i.e. surface to bulk) direction of magnetization transfer, and leads to 2D spectra that are highly asymmetric.

The $^{31}$P 2D exchange spectra for tin pyrophosphate are shown in Fig. 3B. As expected, when the mixing time is 0 s, all the spectral intensity lies along the diagonal. For a 1 s mixing time, the polarization that was generated on the surface is now flowing into the bulk sites, resulting in significant off-diagonal intensities. In agreement with Fig. 2C, the spectra indicate that the relatively broad range of surface shifts exchange with both of the bulk peaks on similar timescales. The spectrum with the longest mixing time

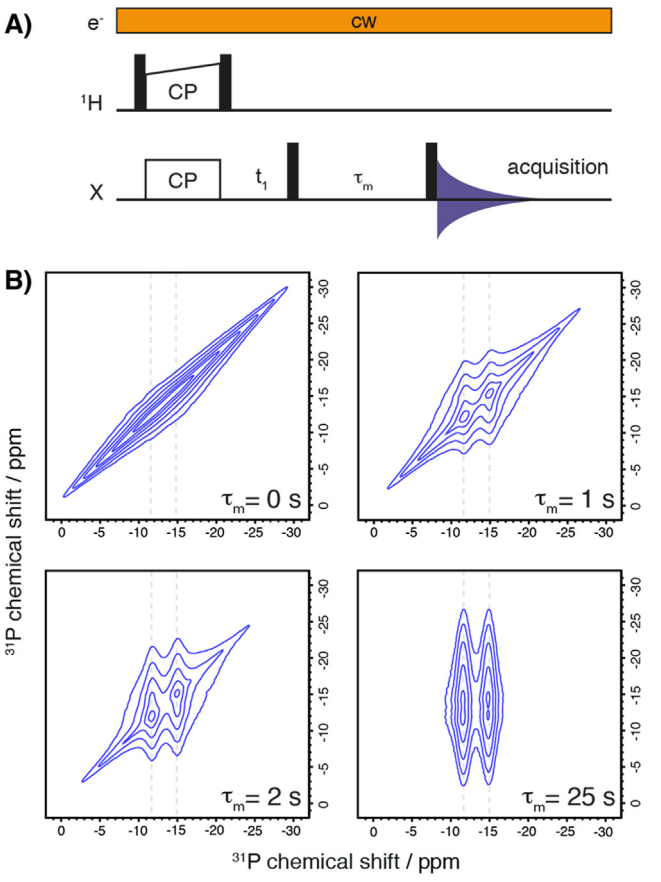


**Fig. 3.** (A) DNP enhanced 2D SD CP-EXSY pulse sequence used to monitor spin diffusion from surface to bulk. (B) Contour plots of DNP enhanced 2D $^{31}$P CP spin diffusion spectra of $Sn_2P_2O_7$ showing only the region of the centerband. The grey dashed lines are at the chemical shift of the two bulk peaks.

shows how after a spin diffusion period of $\tau_m$ = 25 s, all of the polarization that was on the surface has now diffused into the bulk.

In addition, the off-diagonal intensities between the surface resonances close to the bulk resonances in the spectrum appear faster than the off-diagonal intensities between the bulk and the surface resonances furthest away from bulk (-5 and −25 ppm). This suggests either that the rate of transfer to bulk is slower as the chemical shift difference increases, or that there is a relay step through surface sites having resonances closer to the bulk (see Fig. S1).

We note that only a handful of homonuclear surface to bulk correlations in inorganic materials have been reported previously, for example in the context of nanoparticles or battery materials [31,32].

### 3.1.2. $^{119}$Sn spin diffusion in tin dioxide

Efficient hyperpolarization of the bulk $^{119}$Sn atoms in $SnO_2$ was shown previously [10,11]. Here we look into the mechanism of relay from surface to bulk in the same way as for tin pyrophosphate above. The DNP enhanced $^{119}$Sn surface spectrum of $SnO_2$ is shown in Fig. 4A. The surface spectrum of $SnO_2$ is characterized by three notable peaks corresponding to different sites. These signals can be observed in hydroxylated $SnO_2$ nanosheets and have been assigned to different atomic layers [33]. The bulk-like $^{119}$Sn is at −604 ppm (*B*) and the first and second atomic layer, respectively, were assigned chemical shifts of −585 ppm ($S_1$) and −618 ppm ($S_2$). We note that the samples under consideration here are micrometer sized particles.

The $^{119}$Sn 2D spectra of $SnO_2$ with a mixing time of 0 s do not have any cross peaks, as expected (see SI). With a $\tau_m$ = 1 s, the presence of off-diagonal intensity shows that spontaneous $^{119}$Sn-$^{119}$Sn spin diffusion is present. Compared to spin diffusion between $^{31}$P nuclei, $^{119}$Sn-$^{119}$Sn spin diffusion is considerably slower (notably because the natural abundance of $^{119}$Sn is 8.6%), and it takes longer for all of the surface hyperpolarization in $SnO_2$ to transfer to site *B*, corresponding to the bulk of the material.

As each of the surface sites in $SnO_2$ has a relatively well defined chemical shift range, it is possible to look at how the different sites exchange with the bulk. As an example, the region corresponding to transfer from surface site $S_1$ to bulk is more intense than the peak for bulk to surface $S_1$ transfer. This expected due to the predominantly forward transfer of surface hyperpolarization into the bulk of the $SnO_2$ particles due to the strong non-Boltzmann polarization gradient established near the particle surface.

This can be analyzed in more detail with the kinetic model introduced above, this time with three sites, as shown in Fig. 5A. The model considers reversible exchange between all three sites, represented by six rate constants, *k*. Additionally, the model takes into account three relaxation rates, *R* (where $R = 1/T_1$), one for each site. The total kinetic rate matrix can be written as

$$\mathbf{L} = \begin{bmatrix} -(k_{12}+k_{13})-R_{S2} & k_{21} & k_{31} \\ k_{12} & -(k_{21}+k_{23})-R_B & k_{32} \\ k_{13} & k_{23} & -(k_{31}+k_{32})-R_{S1} \end{bmatrix} \quad (4)$$

To find the rate constants representing the observed transfer between the different sites, the integrated areas, ***I***, from the two-dimensional spin diffusion spectra can be fitted to the following matrix equation:

$$\boldsymbol{I}(\tau_m) = \boldsymbol{V}_0 e^{\boldsymbol{L}\tau_m} \quad (5)$$

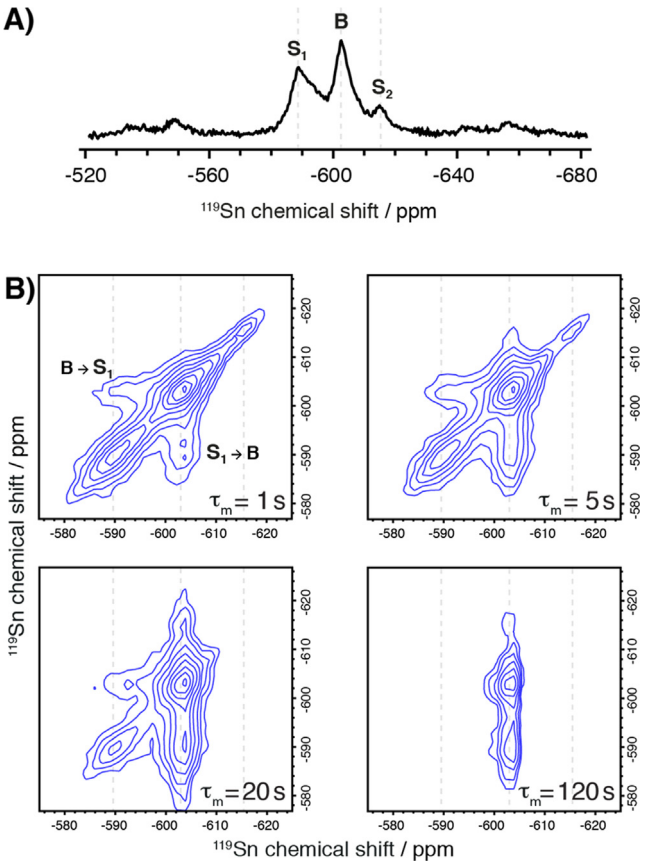


**Fig. 4.** $^{119}$Sn spectra of $SnO_2$ recorded at 9.4 T and 100 K. (A) DNP surface enhanced CP-MAS $^{119}$Sn spectrum of $SnO_2$. B) Contour plots of DNP enhanced $^{119}$Sn spin exchange spectra of $SnO_2$ with different mixing times. The grey dashed lines are at the chemical shifts of the bulk and the two surface sites.

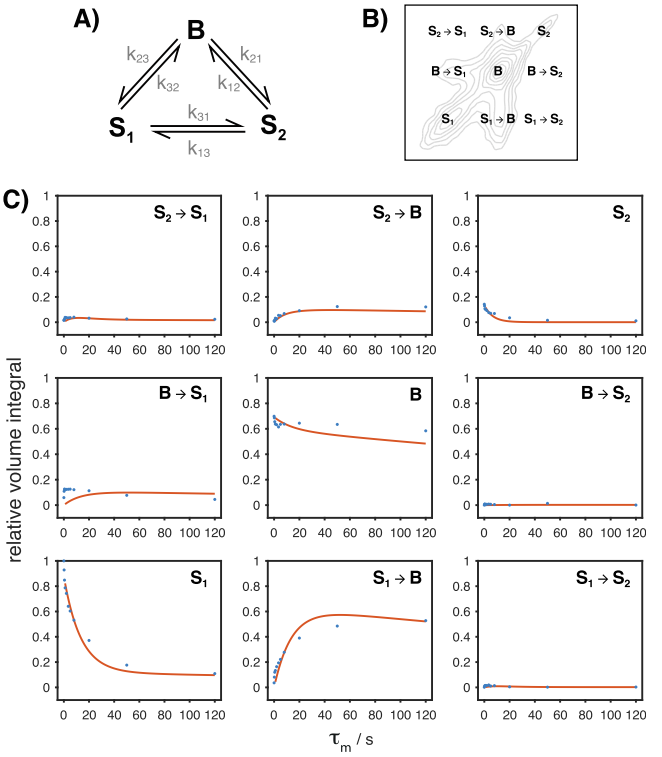


**Fig. 5.** (A) The three-site exchange model used to describe exchange between one bulk site and two surface sites. (B) 2D spectrum marked with the first-order pathway of relay for each peak. (C) Volume integrals of the diagonal and cross peaks from the 2D $^{119}$Sn spectra of $SnO_2$ as a function of mixing time, $\tau_m$. The solid lines are the results of the best fit of the data to the multisite exchange model described in the text.

where $\boldsymbol{V_0}$ is proportional to the volume magnetization before exchange [30,34].

The graphs in Fig. 5 show the volume integral as a function of mixing time for each of the peaks in the 2D $^{119}$Sn-$^{119}$Sn spectra (see Fig. S4 for spectra). In general, the intensity of the observed cross peaks first increases as a function of mixing time and then decreases at longer $\tau_m$ due to spin-lattice relaxation. The diagonal peaks start off at the initial state of the magnetization, before spin diffusion, and they decrease as a function of mixing time as magnetization diffuses away from the site on which it originated.

The observed rate constants of transfer from surface to bulk extracted by fitting the peak volumes to the kinetic model ($k_{12}$ = 0.08 s$^{-1}$ and $k_{32}$ = 0.05 s$^{-1}$) are higher than the observed rate constant of back-transfer to the surface from the bulk ($k_{21}$ = 0.0001 s$^{-1}$ and $k_{23}$ = 0.01 s$^{-1}$). The cross peaks between surface site $S_1$ and surface site $S_2$ are of low intensity, but the curves do show the expected characteristic behavior, and we find observed $k_{13}$ = 0.06 s$^{-1}$ and $k_{31}$ = 0.003 s$^{-1}$ (see SI for details). This suggests that direct communication between the two surface sites occurs on a similar timescale as transfer to the bulk.

The apparent asymmetry in the observed rate constants (i.e. $k_{12} \neq k_{21}$) can be rationalized by the difference in the volume of the surface (lower volume) and bulk (higher volume). The microscopic forward and reverse spin exchange steps should have the same probability in both surface and bulk, but in the low volume of the surface part, a given transfer step is much more likely to lead to transfer to bulk than the reverse process. We note that the asymmetry in the spectra observed here require a difference in the forward and backward rate constants to be explained. This is not the same as asymmetry induced purely by non-equilibrium starting conditions [35,36].

The spin-lattice relaxation rates extracted from the model are $R_{S1} \simeq R_{S2} \simeq 0.01$ s$^{-1}$ and $R_B \simeq 0$ s$^{-1}$is not surprising considering that the longest mixing time is 120 s, and the build-up time of the bulk has been measured to be over 600 s at 8 kHz MAS rate. We also note that there are some systematic errors in the fit (notably for diagonal peak $B$ and cross-peak $B \rightarrow S_1$) which might slightly affect the accuracy of the determination but which will not alter the overall conclusions.

### 3.1.3. $^{31}$P spin diffusion in gallium phosphide

We previously also showed how hyperpolarization from a broad range of surface shifts around the single $^{31}$P bulk resonance of gallium phosphide, GaP, was transferred into the bulk by relay [10].

Fig. 6B shows contour plots of DNP enhanced 2D $^{31}$P spin diffusion spectra of GaP with different mixing times. These spectra indicate two different surface sites (Fig. 6A) transferring hyperpolarization into the bulk, which has a chemical shift of −148 ppm, on a timescale of around 10 s. The off-diagonal intensities representing surface transferring to bulk are observable within one second, and all of the surface polarization has been relayed from both surface sites to the bulk GaP after $\tau_m$ = 10 s. No cross peaks corresponding to bulk going back to surface are observed in these spectra.

Fig. 6C shows cross-sections from the 2D spectra, taken parallel to $\omega_1$. Each cross section contains a diagonal peak centered on the surface resonance at around −5 ppm. It decays monotonically as the mixing time is increased, as polarization is transferred to a region centered at −148 ppm. However, most interestingly, the linewidth of the cross peak at −148 ppm changes significantly with the length of the spin diffusion period, going from over 20 ppm when $\tau_m$ = 1 s to less than 8 ppm at $\tau_m$ = 20 s. This unambiguously indicates that some of the surface polarization that starts at −5 ppm is first transferred to other surface sites in the range −130 to −170 ppm, before then being further transferred to the bulk at −148 ppm (see also Fig. S3).

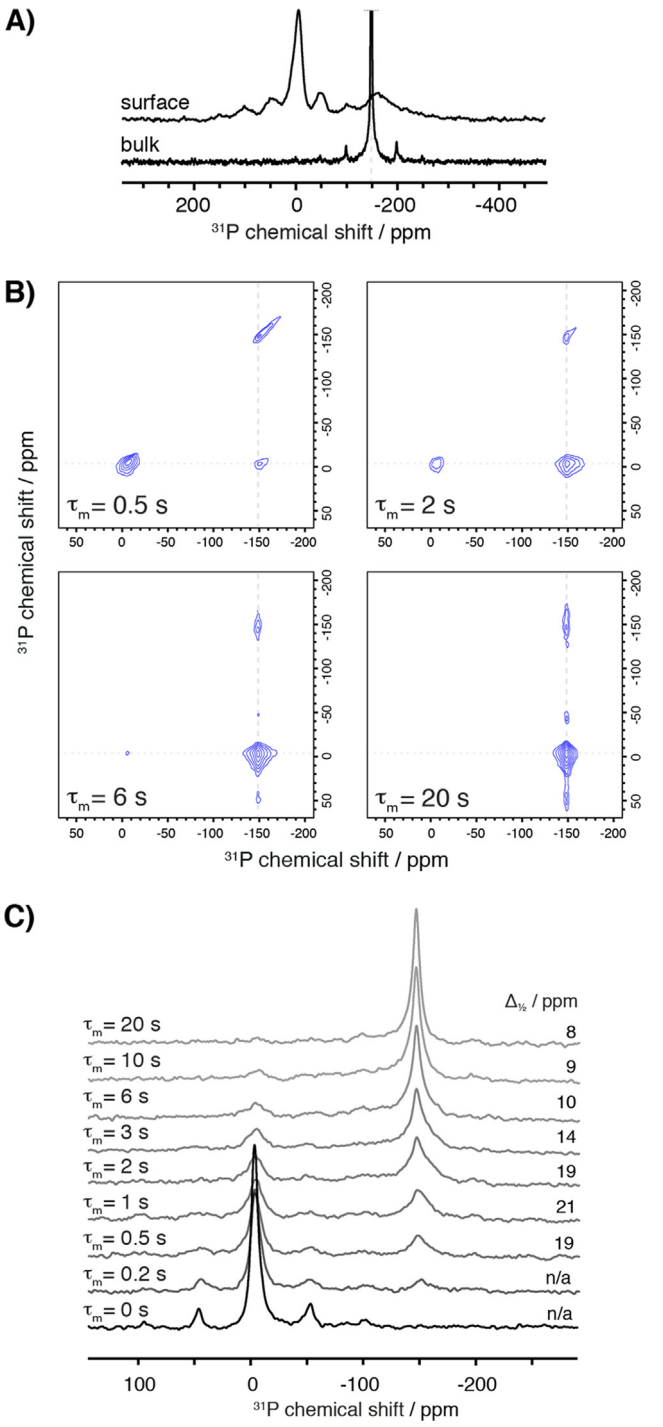


**Fig. 6.** DNP enhanced $^{31}$P spectra of GaP. (A) Surface ($^1$H-$^{31}$P CP) and bulk $^{31}$P spectra of GaP. (B) Contour plots of DNP enhanced $^{31}$P spin exchange spectra of GaP with different mixing times. The vertical dashed line is at the chemical shift of the bulk. C) Cross-sections taken along the dotted line in (B) parallel to $\omega_1$ from the $^{31}$P spin exchange spectra of GaP at different mixing times. The full width at half height $\Delta_{½}$ of the cross peak located around −148 ppm is reported on the right.

### 3.2. Exchange between bulk sites

After looking into the relay process from surface to bulk, we shift the attention to polarization exchange between two or more different bulk sites in the same compound. The approach for studying this is well established and has been used before in the context of spin diffusion [14], the main difference here being that the initial condition for the 2D experiment is prepared with the pulse cooling

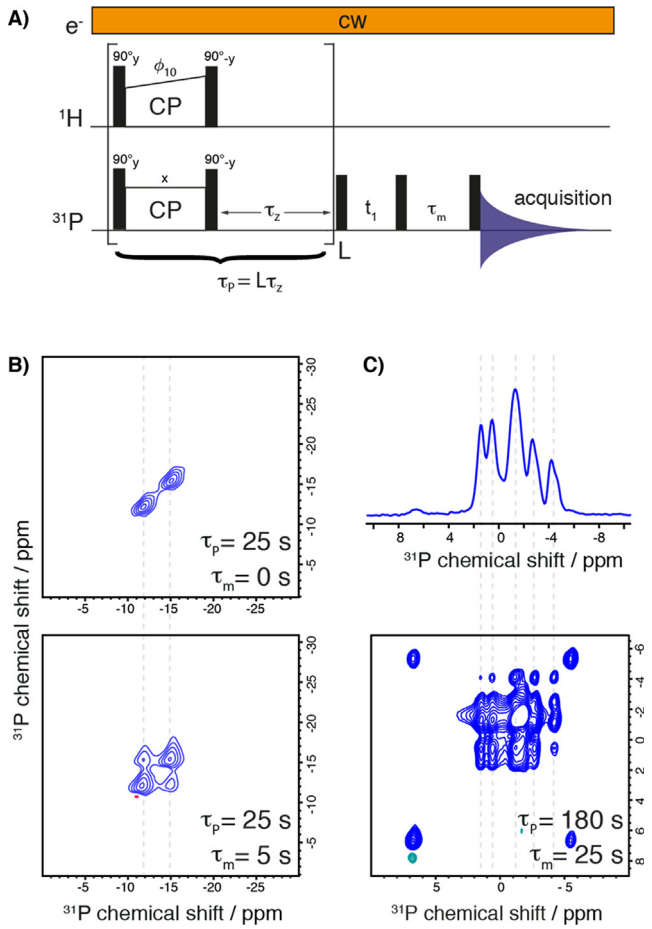


**Fig. 7.** (A) Pulse sequence used in the bulk-bulk 2D spin diffusion experiment. (B) Contour plots of the DNP enhanced $^{31}$P CP spectra of $Sn_2P_2O_7$ showing bulk exchange. (C) $^{31}$P spectrum of neat (not impregnated) $K_4P_2O_7$ above the DNP enhanced $^{31}$P CP two-dimensional spectrum of $K_4P_2O_7$ showing bulk exchange.

[10] method. This DNP enhanced variant of the conventional EXSY pulse sequence is shown in Fig. 7A. Bursts of cross-polarization repeatedly hyperpolarize the surface of the particle, and the polarization moves towards the bulk during a spin diffusion delay $\tau_z$, building up with the number of CP contacts. The advantage of using this strategy rather than direct excitation of the X nucleus is that it can provide higher signal-to-noise ratio for the bulk. Following the preparation of the initial condition, the pulse sequence continues as shown in Fig. 7A with a 2D exchange experiment as described previously for the surface to bulk transfer. After the mixing period, $\tau_m$, the absence or presence of an off-diagonal intensity will determine whether there is exchange/spin diffusion between the two bulk peaks.

### 3.2.1. $^{31}$P spin diffusion in tin pyrophosphate

Fig. 7B shows that polarization transfer between the two bulk sites in tin pyrophosphate happens on the order of a few seconds. In this case, a two-site exchange model where we assume $k_{AB} = k_{BA}$ can be used to determine the observed rate of transfer:

$$\frac{I_{AA}}{I_{AB}} = \frac{1 + \exp(-2k\tau_m)}{1 - \exp(-2k\tau_m)} \quad (6)$$

The ratio of intensities for the diagonal peaks, $I_{AA}$, and cross-peaks, $I_{AB}$, are 1.98 and 1.94, giving an observed exchange rate constant of around $k$ = 0.11 $s^{-1}$. In this case, there is no observable back-transfer to the surface.

### 3.2.2. $^{31}$P spin diffusion in potassium pyrophosphate

Another example of this is shown for the $^{31}$P spectrum of potassium pyrophosphate, $K_4P_2O_7$ (Fig. 7C), which has five isotropic chemical shifts over a range of around 5 ppm [37]. This compound has a $^{31}$P longitudinal relaxation rate of >400 s and, as before, the pulse cooling strategy is used before the mixing period, in order to increase sensitivity.

Cross peaks between the bulk sites in the DNP enhanced 2D bulk exchange spectrum in Fig. 7C are apparent between all the bulk sites (one of the cross peaks is not shown in the contour plot as it is too close to the noise), as well as with the prominent slow-relaxing surface peak at around −1.5 ppm. This indicates that even if the surface hyperpolarization were only channeled into one of the bulk resonances, the rest of the bulk sites would also become hyperpolarized by relay, as the bulk resonances exchange with each other on a timescale that is shorter than the relaxation time of the compound.

## 4. Conclusions

We have shown how two-dimensional spin diffusion experiments can be used to study the pathways of polarization exchange between weakly magnetic nuclei in inorganic materials. In particular, we focus on magnetization transfer from surface sites to bulk under MAS, even in the presence of significant chemical differences. We show this with the $^{31}$P spectra of $Sn_2P_2O_7$, GaP and $K_4P_2O_7$, and the $^{119}$Sn spectra of $SnO_2$. We found that polarization can be transferred from a range of surface sites with different chemical shifts to other surface sites, and to one or more bulk sites on the same time scale.

## Declaration of Competing Interest

The authors declare that they have no known competing financial interests or personal relationships that could have appeared to influence the work reported in this paper.

## Acknowledgements

This work was supported by Swiss National Science Foundation Grant No. 200020_178860.

## Appendix A. Supplementary material

Supplementary data to this article can be found online at https://doi.org/10.1016/j.jmr.2020.106888. All the raw NMR data can be found online at https://doi.org/10.5281/zenodo.4317325.

## References

[1] A.S.L. Thankamony, J.J. Wittmann, M. Kaushik, B. Corzilius, Dynamic nuclear polarization for sensitivity enhancement in modern solid-state NMR, Prog. Nucl. Magn. Reson. Spectrosc. 102 (2017) 120–195.
[2] L. Zhao, A.C. Pinon, L. Emsley, A.J. Rossini, DNP-enhanced solid-state NMR spectroscopy of active pharmaceutical ingredients, Magn. Reson. Chem. 56 (7) (2018) 583–609.
[3] A.J. Rossini, Materials characterization by dynamic nuclear polarization-enhanced solid-state NMR spectroscopy, J. Phys. Chem. Lett. 9 (17) (2018) 5150–5159.
[4] A. Pines, M.G. Gibby, J.S. Waugh, Proton-enhanced NMR of dilute spins in solids, J. Chem. Phys. 59 (2) (1973) 569–590.
[5] A.J. Rossini, A. Zagdoun, F. Hegner, M. Schwarzwälder, D. Gajan, C. Copéret, A. Lesage, L. Emsley, Dynamic nuclear polarization NMR spectroscopy of microcrystalline solids, J. Am. Chem. Soc. 134 (40) (2012) 16899–16908.
[6] P.C.A. van der Wel, K.N. Hu, J. Lewandowski, R.G. Griffin, Dynamic nuclear polarization of amyloidogenic peptide nanocrystals: GNNQQNY, a core segment of the yeast prion protein Sup35p, J. Am. Chem. Soc. 128 (33) (2006) 10840–10846.
[7] A.C. Pinon, U. Skantze, J. Viger-Gravel, S. Schantz, L. Emsley, Core-shell structure of organic crystalline nanoparticles determined by relayed

dynamic nuclear polarization NMR, J. Phys. Chem. A 122 (44) (2018) 8802–8807.
[8] A.C. Pinon, J. Schlagnitweit, P. Berruyer, A.J. Rossini, M. Lelli, E. Socie, M.X. Tang, T. Pham, A. Lesage, S. Schantz, L. Emsley, Measuring nano- to microstructures from relayed dynamic nuclear polarization NMR, J. Phys. Chem. C 121 (29) (2017) 15993–16005.
[9] A. Lesage, M. Lelli, D. Gajan, M.A. Caporini, V. Vitzthum, P. Miéville, J. Alauzun, A. Roussey, C. Thieuleux, A. Mehdi, G. Bodenhausen, C. Coperet, L. Emsley, Surface enhanced NMR spectroscopy by dynamic nuclear polarization, J. Am. Chem. Soc. 132 (44) (2010) 15459–15461.
[10] S. Bjorgvinsdottir, B.J. Walder, A.C. Pinon, L. Emsley, Bulk nuclear hyperpolarization of inorganic solids by relay from the surface, J. Am. Chem. Soc. 140 (25) (2018) 7946–7951.
[11] S. Bjorgvinsdottir, B.J. Walder, N. Matthey, L. Emsley, Maximizing nuclear hyperpolarization in pulse cooling under MAS, J. Magn. Reson. 300 (2019) 142–148.
[12] M.M. Maricq, J.S. Waugh, NMR in rotating solids, J. Chem. Phys. 70 (7) (1979) 3300–3316.
[13] M.E. Halse, A. Zagdoun, J.N. Dumez, L. Emsley, Macroscopic nuclear spin diffusion constants of rotating polycrystalline solids from first-principles simulation, J. Magn. Reson. 254 (2015) 48–55.
[14] D. Suter, R.R. Ernst, Spin diffusion in resolved solid-state NMR Spectra, Phys. Rev. B 32 (9) (1985) 5608–5627.
[15] A. Kubo, C.A. McDowell, Spectral spin diffusion in polycrystalline solids under magic-angle spinning, J. Chem. Soc., Faraday Trans. 1: Phys. Chem. Condens. Phases 84 (11) (1988) 3713–3730.
[16] M. Rosay, L. Tometich, S. Pawsey, R. Bader, R. Schauwecker, M. Blank, P.M. Borchard, S.R. Cauffman, K.L. Felch, R.T. Weber, R.J. Temkin, R.G. Griffin, W.E. Maas, Solid-state dynamic nuclear polarization at 263 GHz: spectrometer design and experimental results, PCCP 12 (22) (2010) 5850–5860.
[17] A. Zagdoun, A.J. Rossini, M.P. Conley, W.R. Gruning, M. Schwarzwalder, M. Lelli, W.T. Franks, H. Oschkinat, C. Coperet, L. Emsley, A. Lesage, Improved dynamic nuclear polarization surface-enhanced NMR spectroscopy through controlled incorporation of deuterated functional groups, Angew. Chem. Int. Ed. Engl. 52 (4) (2013) 1222–1225.
[18] A. Zagdoun, A.J. Rossini, D. Gajan, A. Bourdolle, O. Ouari, M. Rosay, W.E. Maas, P. Tordo, M. Lelli, L. Emsley, A. Lesage, C. Coperet, Non-aqueous solvents for DNP surface enhanced NMR spectroscopy, Chem. Commun. 48 (5) (2012) 654–656.
[19] M. Rosay, Ph.D. Thesis, Massachusetts Institute of Technology, Cambridge, MA, 2001.
[20] D.J. Kubicki, A.J. Rossini, A. Purea, A. Zagdoun, O. Ouari, P. Tordo, F. Engelke, A. Lesage, L. Emsley, Amplifying dynamic nuclear polarization of frozen solutions by incorporating dielectric particles, J. Am. Chem. Soc. 136 (44) (2014) 15711–15718.
[21] D. Massiot, F. Fayon, M. Capron, I. King, S. Le Calve, B. Alonso, J.O. Durand, B. Bujoli, Z.H. Gan, G. Hoatson, Modelling one- and two-dimensional solid-state NMR spectra, Magn. Reson. Chem. 40 (1) (2002) 70–76.
[22] V.V. Chernaya, A.S. Mitiaev, P.S. Chizhov, E.V. Dikarev, R.V. Shpanchenko, E.V. Antipov, M.V. Korolenko, P.B. Fabritchnyi, Synthesis and investigation of Tin(II) pyrophosphate Sn2p2o7, Chem. Mater. 17 (2) (2005) 284–290.
[23] P. Amornsakchai, D.C. Apperley, R.K. Harris, P. Hodgkinson, P.C. Waterfield, Solid-state NMR studies of some Tin(II) compounds, Solid State Nucl. Magn. Reson. 26 (3–4) (2004) 160–171.
[24] N.A. Prisco, A.C. Pinon, L. Emsley, B.F. Chmelka, Quantitative Scaling analyses for hyperpolarization transfer across a spin-diffusion barrier and into bulk solid media. Transfer across Dissimilar Interfaces, 2020 (in press).
[25] J. Viger-Gravel, A. Schantz, A.C. Pinon, A.J. Rossini, S. Schantz, L. Emsley, Structure of lipid nanoparticles containing siRNA or mRNA by dynamic nuclear polarization-enhanced NMR spectroscopy, J. Phys. Chem. B 122 (7) (2018) 2073–2081.
[26] S.E. Day, M.I. Kettunen, F.A. Gallagher, D.E. Hu, M. Lerche, J. Wolber, K. Golman, J.H. Ardenkjaer-Larsen, K.M. Brindle, Detecting tumor response to treatment using hyperpolarized C-13 magnetic resonance imaging and spectroscopy, Nat. Med. 13 (11) (2007) 1382–1387.
[27] P.W. Kuchel, D. Shishmarev, Dissolution dynamic nuclear polarization NMR studies of enzyme kinetics: setting up differential equations for fitting to spectral time courses, J. Magnetic Reson. Open 1 (2019).
[28] J. Jeener, B.H. Meier, P. Bachmann, R.R. Ernst, Investigation of exchange processes by 2-dimensional NMR-spectroscopy, J. Chem. Phys. 71 (11) (1979) 4546–4553.
[29] N.M. Szeverenyi, M.J. Sullivan, G.E. Maciel, Observation of spin exchange by two-dimensional fourier-transform C-13 cross polarization-magic-angle spinning, J. Magn. Reson. 47 (3) (1982) 462–475.
[30] E.W. Abel, T.P.J. Coston, K.G. Orrell, V. Sik, D. Stephenson, Two-dimensional NMR exchange spectroscopy - quantitative treatment of multisite exchanging systems, J. Magn. Reson. 70 (1) (1986) 34–53.
[31] S. Haber, M. Leskes, What can we learn from solid state NMR on the electrode-electrolyte interface?, Adv. Mater. 30 (41) (2018).
[32] M.P. Hanrahan, Y.H. Chen, R. Blome-Fernandez, J.L. Stein, G.F. Pach, M.A.S. Adamson, N.R. Neale, B.M. Cossairt, J. Vela, A.J. Rossini, Probing the surface structure of semiconductor nanoparticles by DNP SENS with dielectric support materials, J. Am. Chem. Soc. 141 (39) (2019) 15532–15546.
[33] J.C. Chen, X.P. Wu, L. Shen, Y.H. Li, D. Wu, W.P. Ding, X.Q. Gong, M. Lin, L.M. Peng, Identification of different tin species in SnO2 nanosheets with Sn-119 solid-state NMR spectroscopy, Chem. Phys. Lett. 643 (2016) 126–130.
[34] C.L. Perrin, T.J. Dwyer, Application of 2-dimensional NMR to kinetics of chemical-exchange, Chem. Rev. 90 (6) (1990) 935–967.
[35] S. Caldarelli, L. Emsley, Intrinsic asymmetry in multidimensional solid-state NMR correlation spectra, J. Magn. Reson. 130 (2) (1998) 233–237.
[36] M. Kock, C. Griesinger, Fast noesy experiments – an approach for fast structure determination, Angew. Chem.-Int. Ed. 33 (3) (1994) 332–334.
[37] S. Hayashi, K. Hayamizu, High-resolution solid-state P-31 NMR of alkali phosphates, Bull. Chem. Soc. Jpn. 62 (10) (1989) 3061–3068.